HHS Public Access

Author manuscript

ACS Infect Dis. Author manuscript; available in PMC 2019 June 08.

Published in final edited form as:

ACS Infect Dis. 2018 June 08; 4(6): 904–911. doi:10.1021/acsinfecdis.7b00263.

Measuring the global substrate specificity of mycobacterial serine hydrolases using a library of fluorogenic ester substrates

Braden Bassett[a], **Brent Waibel**[a], **Alex White**[a], **Heather Hansen**[a], **Dominique Stephens**[a], **Andrew Koelper**[a], **Erik M. Larsen**[a], **Charles Kim**[b], **Adam Glanzer**[a], **Luke D. Lavis**[b], **Geoffrey C. Hoops**[a], and **R. Jeremy Johnson**[a,*]

[a]Department of Chemistry and Biochemistry, Butler University, 4600 Sunset Ave., Indianapolis, IN 46208-3443 (USA)

[b]Howard Hughes Medical Institute, Janelia Research Campus, 19700 Helix Dr., Ashburn, VA 20147-2439 (USA)

Abstract

Among the proteins required for lipid metabolism in *M. tuberculosis* are a significant number of uncharacterized serine hydrolases, especially lipases and esterases. Using a streamlined synthetic method, a library of immolative fluorogenic ester substrates were expanded to better represent the natural lipidomic diversity of *Mycobacterium*. This expanded fluorogenic library was then used to rapidly characterize the global structure activity relationship (SAR) of mycobacterial serine hydrolases in *M. smegmatis* under different growth conditions. Confirmation of fluorogenic substrate activation by mycobacterial serine hydrolases was performed using nonspecific serine hydrolase inhibitors and reinforced the biological significance of the SAR. The hydrolases responsible for the global SAR were then assigned using gel-resolved activity measurements and these assignments used to rapidly identify the relative substrate specificity of previously uncharacterized mycobacterial hydrolases. These measurements provide a global SAR of mycobacterial hydrolase activity, a picture of cycling hydrolase activity, and a detailed substrate specificity profile for previously uncharacterized hydrolases.

Keywords

Serine hydrolases; Structure activity relationship; Tuberculosis; Fluorogenic substrates; *Mycobacterium tuberculosis*; Substrate specificity

[*]Corresponding author: rjjohns1@butler.edu. Phone: 317-940-9062.

Supporting Information

Supplementary data associated with this article can be found in the online version at: Detailed experimental methods, including complete synthetic characterization of novel fluorogenic substrates. Expanded whole cell, secretion, and lysate activity measurements. LC-MS peptide fragments and alignment data.

ORCID

Luke D. Lavis: 0000-0002-0789-6343

R. Jeremy Johnson: 0000-0003-2694-3915

Notes

The authors declare no competing financial interest.

Tuberculosis (TB) caused by infection by *Mycobacterium tuberculosis* (*Mtb*) is the deadliest infectious disease worldwide.[1] One difficulty in treating TB infections is the ability of *Mtb* to convert from an active infectious state to a latent dormant state within a patient's lungs.[2] Survival of *Mtb* within this dormant state is facilitated by a variety of factors, including complex metabolic shuttling and a battery of mycobacterial enzymes used to scavenge for host cell lipids and nutrients.[3] Among the enzymes involved in breaking down host cell nutrients are serine hydrolases, especially esterases and lipases.[4, 5] Based on their disease regulated expression and activity, mycobacterial serine hydrolases have been proposed as novel drug targets.[6, 7] Using activity based protein profiling (ABPP), shifts in serine hydrolase activity were correlated with growth conditions observed during dormancy, including hypoxia and nutrient starvation.[8–10] Through these studies, over 80 discrete proteins were identified with serine hydrolase activity and among those hydrolases the activity of over 30% shifted in relation to dormant growth conditions.[8–10] Each of these studies also found that serine hydrolase expression levels were not a good predictor of relative activity changes.[8–10]

The expansion of serine hydrolase activity in *M. tuberculosis* in comparison to humans or other common bacteria has also been proposed to encode unique chemical reactivity or substrate specificity that could serve as a fingerprint for demarcating dormant and active *Mtb* infections.[9, 11, 12] This expansion is exemplified by the hormone sensitive lipase (HSL) superfamily where only one human HSL superfamily member is expanded to nine HSL members in *Mtb* with each member showing distinct substrate reactivity dependent on slight structural variations.[7, 13] This hypothesis of unique substrate specificity within *Mtb* serine hydrolases is further supported by the diverse natural lipodomic substrates constructed by *Mtb*.[3] The complex *Mtb* cell wall, for example, contains mycobacterial specific fatty acids including phthioceranic acids, mycolipanolic acids, mycolipenic acids, mycocerosic acids, and mycosanoic acids.[14–17] Mycobacterial hydrolases are known to regulate mycomembrane composition, to bind the common phthiocerol core, and to be encoded in operons with other fatty acid metabolism genes, supporting the potential for mycobacterial hydrolases to be active against these mycobacterial substrates.[10, 18, 19]

Building on this hypothesis of unique mycobacterial serine hydrolase activity, we streamlined the synthesis of a library of fluorogenic ester substrates and utilized this modular synthesis to assemble novel substrates mimicking the natural branching, substitution, and saturation patterns of mycobacterial fatty acids. Using *M. smegmatis* as a model organism, we then used this library to characterize the global substrate specificity of mycobacterial serine hydrolases under normal and nutrient starvation growth conditions and also to identify global structure activity relationships related to its hydrolase activity. Using in-gel hydrolase measurements and mass spectrometry, we then began to deconvolute this complex global substrate specificity and to assign unique reactivity to individual mycobacterial hydrolases.

To track mycobacterial hydrolase activity, we used a library of acyloxymethyl ether fluorescein derivatives whose inherently bright fluorescence is masked by various ester reactive moieties.[20, 21] These acyloxymethyl ether fluorescein derivatives provide low background fluorescence, fast activation kinetics, and space the reactive ester away from the

bulky fluorophore to reduce its interference in kinetic measurements.[22–25] The previous synthetic procedure for these fluorogenic substrates provided complex mixtures of mono- and dialkylated and acylated products that required multistep separations and provided minimal yields (Figure 1A).[20, 23] To increase the throughput of fluorophore synthesis, a streamlined synthetic method was designed in which fluorescein is first alkylated in two steps and then a stable dichloromethyl ether fluorescein intermediate (DCMEF) is derivatized in one common step to a library of new fluorogenic substrates (Figure 1B). This new synthesis eliminates contaminating by-products, greatly simplifying final purification, significantly increasing yields (50-95%), and facilitating rapid synthesis of the fluorogenic ester library. Using this streamlined synthesis, we expanded our previous fluorogenic library (Figure 1C) to systemically investigate the SAR of alkyl ester branching at positions α, β, and γ to the carbonyl (**6-12**) and of introducing further polar substituents (**15-16, 22**) and unsaturation (**18**) while maintaining representative substrates from across standard serine hydrolase superfamilies (**1-5**, **19-21**, **23-24**).[23, 24]

Using this library, we then investigated the global substrate specificity of actively growing *Mycobacterium smegmatis* (*Msm*) under standard growth conditions. We chose *Msm* for this analysis because *Msm* is the closest non-pathogenic evolutionary relative to *Mtb* and has a higher number of protein orthologues to *Mtb* than other pathogenic mycobacteria, including *M. leprae* and *M. abscessus*.[26] The mycobacterial activities requiring serine hydrolase activity, including dormancy and lipid body accumulation, are also conserved between *Msm* and *Mtb* as are the majority of serine hydrolases.[27, 28] Initial measurements in actively growing cultures showed that fluorogenic substrate activation was linear over an extended period (6 hours) with very low background hydrolysis for the majority of substrates (Figure 2A and Figure S1). This low background fluorescence permitted accurate kinetic measurements for weakly activated substrates like tertiary esters (**23-24**), allowing the identification of low reactivity present within *Msm* (Figure 2C). Based on the linearity, global measurements were shortened to the first hour and activation rates were corrected based on the background hydrolysis of each substrate under the same conditions (Figure 2B). In addition, the irreversible general serine hydrolase inhibitor, phenylmethylsulfonyl fluoride (PMSF), was included in each measurement at a subgrowth inhibition concentration (1 mM) to confirm that activation patterns were dependent on serine hydrolase activity (Figure 2D, 2E and S1).

The global substrate specificity map showcases a few substrates that are significantly more activated than the rest of the library (Figure 2C). Focusing on substrates **1-5**, a simple SAR can be drawn correlating increasing alkyl chain length with decreasing reactivity (Figure 2C). A similar SAR is then recapitulated in substrates **13-15** illustrating a strong preference for the shortest alkyl ether ester substrates (Figure 2C). These SAR patterns are in contrast to *in vitro* serine hydrolase substrate specificity measurements with similar fluorogenic substrates, which have shown maximal catalytic activity of diverse serine hydrolases for four and six carbon alkyl substrates.[13, 23, 24, 29] The highest activity for substrates **13-15**, however, matches with the *in vitro* characterization of two mycobacterial hydrolases (Rv0045c and LipW), which showed a preference for these polar alkyl ether esters and reinforced their proposed biological roles in metabolism.[13, 24] These substrates also have

some of the highest background hydrolysis rates (Figure S1) and with their polar substituents alpha to the carbonyl were hypothesized to be more labile to hydrolysis.[13] In comparison to the high activation of these polar mycobacterial substrate mimics (**13**-**15**; **22**), nonpolar mycobacterial substrate mimics (**6**-**12**; **18**), irrespective of length, branching, and substitution, showed the lowest levels of substrate activation (Figure 2C).

Importantly, the majority of the substrate activation is inhibited by PMSF with a few interesting exceptions (Figure 2C). Although small and general, PMSF is known to poorly inhibit esterase enzymes preferring small substrates like **1** and **13**.[30] This inhibition pattern for PMSF is reflected in the substrate specificity profiles against *Msm*, as PMSF only moderately inhibits activation of substrate **1** (Figure 2D), but shows near full inhibition of substrate **3** (Figure 2E). The overlap of our PMSF inhibition pattern with the previously observed specificity of PMSF provides preliminary evidence that our global substrate specificity patterns reflect the natural substrate specificity of serine hydrolases in *Msm*.

Based on this initial specificity pattern, we then set out to address a few questions about mycobacterial serine hydrolase expression and regulation using the expanded fluorogenic substrate library. First, we determined whether substrate activation was attributable to secreted hydrolases. Using culture media extracted from actively growing *Msm* cultures, secreted and actively growing hydrolase activity were compared (Figure S2). Based on this analysis, the majority of substrates showed no activation from secreted hydrolases with only substrates **13**, **15**, and **22** having measurable activity in growth media. This low activity likely reflects the low number and concentration of expected secreted hydrolases with only 6 such hydrolases found by proteomic analysis.[31] However, multiple of these secreted hydrolases play key roles in the virulence and host-pathogen interactions of *M. tuberculosis* and so a more sensitive methodology for detection could have therapeutic applications.[32, 33]

Next, we wanted to determine if hydrolase activity shifted in relation to dormant growth conditions (Figure 3 and Figure S3). Specifically, we tested shifts in hydrolase activity in relation to nutrient starvation under which lipolysis rates and hydrolase activity are correlated.[8, 9, 34] Mycobacterial lysates were first prepared to allow time point dependent measurements of hydrolase activity. The activation profile from the actively growing cultures (Figure 2) and the mycobacterial lysates (Figure S3) overlapped very closely, reaffirming that measured hydrolase activity in actively growing cultures (Figure 2) was not due to secreted hydrolases (Figure S2). Some of the activation profile in the lysates does shift with increased activation of longer alkyl substrates **(5** and **6**), branched substrates (**11** and **12**), and alkyl ether substrates (**13**-**16**) in lysates, indicating the presence of cytosolic hydrolases in the lysates that were not accessible in measurements of actively growing cultures.

Comparing mycobacterial hydrolase activity over a time course of nutrient starvation from 30 minutes to 28 hours, overall hydrolase activity increased immediately after nutrient starvation in the 0.5 – 2 hour time points (Figure 3). This increase in hydrolase activity was conserved across a large number of substrates with highest activity for the majority of substrates after 30 minutes of nutrient starvation. This rapid increase suggests global upregulation of hydrolase activity in relation to nutrient starvation and an initial rapid

cellular response to the stress of nutrient starvation. This pattern of stress dependent serine hydrolase activation in response to nutrient starvation matches with the disappearance of intracellular lipid bodies, which are lipid rich deposits used to sustain growth during dormancy and whose breakdown and synthesis requires significant serine hydrolase activity.[34–36]

The majority of the hydrolase activity then cycled back down over 4 – 8 hours post nutrient starvation (Figure 3A). Increased hydrolase activity then returned between 16 – 28 hours, indicating a secondary response to nutrient starvation. Many of the substrates upregulated between 0.5 – 2 hour were also upregulated at 28 hours, suggesting similar patterns of hydrolase activation under these two regimes. Yet unique substrates (**5**, **10**-**11**, **19**-**20**) showed only activation under the secondary nutrient starvation response and may indicate new hydrolases expressed only upon prolonged nutrient starvation. A small subsection of substrates (**4**, **15**, **19**-**20**) also showed increased expression at 0.5 – 2 hours and again at 16 hours.

Dissecting this SAR (Figure 3B) by structural class shows that all small esters within each subclass of hydrolase substrates (Figure 1C), irrespective of branching or substitutions, were primarily activated immediately after nutrient starvation (0.5 – 2 hrs). This skewed distribution toward smaller substrates indicates that a high number of carboxylesterase hydrolases are expressed in immediate response to nutrient starvation. In comparison, only the longest and largest substrates within each subclass (**5** within linear alkyl esters; **10** and **11** within branched alkyl esters; and **21** within cycloalkyl esters) were differentially activated at only 16 hr, suggesting the expression of more lipases with a preference for longer, bulkier, hydrophobic esters after extended nutrient starvation. Reaffirming this two regime carboxylesterase and lipase expression pattern, substrates of intermediate length and size (**4**, **12**, **15**, **19**-**20**) showed combined activity at 0.5 hrs and 16 hrs, suggesting immediate activation (0.5 – 2 hrs) of broad spectrum carboxylesterases and long term activation of lipases (Figure 3B). The differential preference for substrate size and bulk at these two time points post nutrient starvation represents a potential starting point for identifying a hydrolase signature for demarcating dormant versus active mycobacterial infections. In comparison to normal growth conditions, nutrient starvation showed more activity toward mycobacterial specific lipids where the longest, branched chain esters (**10**-**12**) were differentially activated after prolonged nutrient starvation (Figure 3B). Previous extensions of fluorogenic hydrolase substrates from two-carbon esters to four-carbon and eight-carbon ester substrates showed similar shifts in activation patterns and allowed for the identification of an *Mtb* enzyme (Culp1; Rv1984c) with differential activity for longer chain esters.[11]

These global measurements of mycobacterial serine hydrolase activity allowed us to identify patterns for proteome-wide substrate specificity, to localize hydrolase activity, and to quantitate changes in hydrolase activity in response to nutrient starvation. This analysis provided novel insight about the global regulation and cycling of serine hydrolase activity and the global substrate specificity of mycobacterial serine hydrolases. Each of the individual activation patterns, however, likely represents the aggregation of signals from multiple hydrolases. To deconvolute these patterns, we took advantage of in-gel analysis methodology to pinpoint individual enzymes involved in the global patterns of activation

(Figure 4).[9, 11] For this analysis, individual substrates were incubated with Native-PAGE separated lysates and hydrolases identified by mass spectrometry based peptide sequencing.

For the simplest substrate (**1**), six individual hydrolases were identified with 5 of 6 hydrolases having direct homologues in *Mtb* (Figure 4A). Besides strong peptide overlap (Table S1), hydrolase assignments were reinforced by correlation between the assignments and expected separation variables on Native-PAGE, including isoelectric point and molecular weight (Figure 4A). Each of these hydrolases contains the classic G-x-S-x-G motif designating a serine hydrolase, but they come from various serine hydrolase protein families, including amidohydrolases (*MSMEG_4773* and *MSMEG_2232*), lip family hydrolases (*MSMEG_5271* and *MSMEG_4680*), and uncharacterized hydrolases (*MSMEG_2074* and *MSMEG_1308*). Among these hydrolase families, Lip family hydrolases were previously identified as highly active by in-gel activity measurements and show interesting variation in activity across mycobacterial growth conditions.[7, 9] These six identified hydrolases are, however, not responsible for the differential substrate activity at 16 hours post nutrient starvation (Figure 4B), as no in-gel activity was observed for substrates differentially activated at 16 hour post nutrient starvation (**10**-**12**, **21**) (Figure 3B). Future in-gel identification of this hydrolase activity will require additional sample separations or analyses.[37–39]

Expanding in-gel analysis across the entire substrate library, all 24 substrates were analyzed against the same mycobacterial lysate (Figure 4B and Figure S2). Analysis conditions were optimized to show the clearest number of bands for each substrate and incubation times were slightly varied between each substrate with the majority of substrates imaged at 60 min post incubation.[9, 11] The in-gel analysis provides a qualitative (but not quantitative) picture of the differential hydrolase activity toward each substrate. This analysis provides new information about the differential substrate specificity of the six previously uncharacterized mycobacterial hydrolases. For instance, comparing increasing alkyl chain lengths (**1**-**5**) shows that *MSMEG_2074*, which is the strongest band with substrate **1** shows relatively high activity for only the smallest alkyl ester substrates (**1** and **2**) with only minor residual relative activity with longer carbon chains even with increased incubation times (Figure 4B). This matches with the observed expression of the *Mtb* homologue (*Rv0272c*) in relation to diamide treatment and suggests a small amidohydrolase substrate as its natural biological substrate.[40] In contrast, the other proposed amidohydrolase (*MSMEG_4773*) shows increasing relative activity toward longer chain substrates with the highest relative activity of any of the six hydrolases against substrates **3**-**5**, **13**-**14**, and **16**-**17**. This in-gel analysis also provides biological substrate clues about previously uncharacterized hydrolases, such as *MSMEG_1308*, which has higher relative preferences for small, branched substrates like **16** and **17**. The current in-gel analysis, however, only provides a snapshot of the over 80 serine hydrolases previously identified by ABPP,[9, 10, 41] as only hydrolases within a narrow size and pI range are observed on the gel. The number of hydrolase bands observed in our in-gel analysis, however, matches with previous in-gel measurements across mycobacterial species.[9, 11] The current analysis also expands on previous in-gel analysis to provide substrate specificity comparisons for the six identified hydrolases and this analysis can now be expanded across growth conditions and strains to identify shifts in hydrolase activity.[9, 11, 12]

Using the combination of our fluorogenic substrate library and genetic tools available in *M. smegmatis*, including CRISPR/Cas9 knockdown strains targeting key mycobacterial hydrolases,[5, 42, 43] we are working to deconvolute the specific hydrolases responsible for fluorogenic ester activation.

Conclusions

Mycobacterial serine hydrolases represent a broad, but biologically significant enzyme superfamily with promising therapeutic and diagnostic applications.[9, 28] Using a streamlined synthetic method, we have refined and expanded a library of fluorogenic hydrolase substrates to target interesting substrate specificity patterns in *Msm* (Figure 1). Applying this library to various biological questions, we showed a global SAR exists in actively growing *Msm* with preferences for short and slightly polar substrates (Figure 2). This global hydrolase activity was then tracked based on protein localization, PMSF inhibition profiles, and growth conditions to provide dynamic information about shifts in hydrolase activity (Figures 2, Figure 3 and Figure S2). In-gel analysis allowed us to assign the differential hydrolase activation to individual serine hydrolases and to provide novel substrate specificity comparisons between known and previously uncharacterized serine hydrolases (Figure 4). These methodologies can now be applied as molecular diagnostics to identify novel hydrolase activity for therapeutics or to refine mycobacterial specific ester prodrugs.[6, 9, 44] The fluorogenic SAR library also provides a novel approach for finding biological substrates for uncharacterized hydrolases (Figure 4B).

Methods

Basic synthesis methods

The synthesis of compounds (**1**),[20] (**2**, **17**, **19**, **23-24**),[21] (**3-5**),[22] and (**13-14**, **20-21**)[23] via scheme A (Figure 1A) has been previously described. Unless otherwise noted, all chemicals were purchased from Sigma Aldrich and used without further purification. All reactions were monitored using Macherey-Nagel analytical thin layer chromatography (TLC) plates (POLYGRAM® SIL G/UV_{254}, polyester back). Nuclear magnetic resonance (NMR) spectra were obtained at Butler University with a 400 MHz Bruker Bruker Biospin Avance III HD 400 operating at 400.19 MHz for ^{1}H and 100.64 MHz for ^{13}C. High resolution mass spectrometry (HRMS) was performed with electrospray ionization (ESI) by the Mass Spectrometry facility at Indiana University using an Agilent 1200 HPLC-6130 MSD mass spectrometer. Detailed synthetic methods and synthetic characterization are provided in the Supporting Information.

Mycobacterium smegmatis culture conditions

M. smegmatis m^2 155 (ATCC) was cultured in Middlebrook 7H9 broth (Himedia) supplemented with 0.1% (v/v) Tween 80, 0.4% (v/v) glycerol, and 10% (v/v) ADC (albumin, dextrose, catalase from Himedia). Cultures were incubated at 37 °C with rapid shaking (225 RPM). Growth curves in the presence of PMSF were obtained through recording OD_{600} measurements every 30 min for a standard culture and PMSF (1 mM) containing cultures.

Mycobacterium smegmatis whole-cell assay preparation

M. smegmatis cultures were grown overnight to full density, then serial dilutions were performed to create multiple cultures, which were incubated 15-18 hours. Cultures were then tested for log phase (OD_{600} = 0.5 - 1.0) and if in log phase, one culture was subsequently selected for the assay. The culture was diluted to an OD_{600} of 0.09 in Middlebrook broth. Enzymatic activity of the *M. smegmatis* cultures were measured using fluorogenic substrates in a 96-well plate assay. Fluorogenic substrates were diluted from 10 mM in DMSO stock solutions to 2 μM preparations in 1X PBS buffer. Cell cultures (100 μL) were incubated with fluorogenic substrate solutions (100 μL) in triplicate at 37 °C on a Biotek Synergy H1 multimode plate reader. Fluorescence change (λ_{ex} = 485 nm, λ_{em} = 528 nm) was converted to molar concentrations with a fluorescein standard curve. Spontaneous fluorescent activation was measured simultaneously in triplicate with a fluorogenic substrate solution (100 μL) mixed with Middlebrook without *M. smegmatis* culture (100 μL). An additional control of cell culture (100 μL) with 1 mM PMSF and a fluorogenic substrate solution (100 μL) was also simultaneously measured on each plate. The fluorescence change was converted to molar concentrations using a fluorescein standard curve in PBS (100 nM – 1.56 nM), whose fluorescence was measured simultaneously in triplicate.

Mycobacterium smegmatis lysate preparation

A larger *M. smegmatis* culture (100 mL) was grown at 37 °C and 225 RPM to an OD_{600} between 0.5 and 1.0 for active exponential growth and pelleted by centrifugation at 10,000*g* for 10 minutes and 4 °C. For standard lysate preparation, this pellet was then suspended in 1X PBS (3 mL) and lysed through sonication. Sonication was achieved by 6x 30 s cycles of sonication at 60 Hz with 60 sec of rest on ice between cycles. For time variable lysate samples, the pellet was suspended in 100 mL 1X PBS and incubated at 37 °C with rapid shaking (225 RPM) for the nutrient depravation time (30 minutes-28 hours). As the time variable was reached, the culture was pelleted again, suspended in 3 mL of 1X PBS and lysed using the identical sonication procedure. The concentration of protein in the lysate was determined by measuring the absorbance of the lysates in triplicate using the BCA protein assay microplate protocol (Pierce). Lysates were then frozen at -20 °C.

Mycobacterium smegmatis lysate assay preparation

M. smegmatis lysates were diluted in 1X PBS (150 μg/mL). The procedure for measuring hydrolase activity in lysates was similar to the whole cell assay with the differences described. Cell lysates (100 μL) were incubated with fluorogenic substrate solutions (100 μL). Spontaneous fluorescent activation was accounted for with a fluorogenic substrate solution (100 μL) with PBS (100 μL).

Mycobacterium smegmatis enzyme secretion assay preparation

M. smegmatis was cultured and diluted to the same specifications as in the whole cell assay preparation. The diluted culture was pelleted at 10,000*g* at 4 °C for 10 min and the supernatant collected. The procedure for measuring secreted hydrolase activity was similar to the whole cell assay with the differences described. Cell culture supernatant (100 μL) was incubated with fluorogenic substrate solutions (100 μL).

Mycobacterial smegmatis in-gel activity

M. smegmatis lysates (12 μg) were resolved by native gel electrophoresis (Novex WedgeWell 4-20% Tris-Glycine Gel; Invitrogen) in 1X Tris-Glycine buffer. Gels were run at 200 V for 90 min surrounded by ice. Gels were then separated into lanes prior to soaking in 1X PBS with 3 μM of fluorogenic substrates for 20-60 minutes, optimized per substrate based on background decay (Figure 4B). Gels were imaged with a fluorescence imager (FluorChem Q by Protein Simple, excitation = 475 nm, emission = 537 nm). Fluorogenic bands were excised and sent for LC-MS/MS analysis at Applied Biomics (Hayward, CA). Samples were analyzed by in-gel trypsin digestion, desalting, and MALDI-TOF/TOF analysis using an Applied Biosystems Proteomics Analyzer. Combined MS and MS/MS spectra were matched to the *M. smegmatis* mc^2 155 proteome using GPS Explorer software equipped with the MASCOT search engine. Proteins identified along with their peptide lists and coverages are given in Table S1.

Supplementary Material

Refer to Web version on PubMed Central for supplementary material.

Acknowledgments

R.J.J., A.W., A.K., and E.M.L were supported by a grant from the National Institutes of Health (NIH 1 R15 GM110641-01A1). C.K. and L.D.L. were supported by the Howard Hughes Medical Institute. We thank Ryan Mughmaw and CH432 students for assistance with preliminary fluorogenic substrate synthesis.

Abbreviations

ABBP	activity based protein profiling
ADC	albumin dextrose catalase
DCMEF	dichloromethyl ether fluorescein
ESI	electrospray ionization
HRMS	high resolution mass spectrometry
HSL	hormone sensitive lipase
LC-MS	liquid chromatography – mass spectrometry
MALDI-TOF	matrix assisted laser desorption – time of flight
Msm	*Mycobacterium smegmatis*
Mtb	*Mycobacterium tuberculosis*
Native-PAGE	native-polyacrylamide gel electrophoresis
NMR	nuclear magnetic resonance
PBS	phosphate buffered saline

PMSF	phenylmethylsulfonyl fluoride
RPM	revolutions per minute
SAR	structure activity relationship
SE	standard error
TB	tuberculosis
TLC	thin layer chromatography

References

1. World_Health_Organization. Tuberculosis Facts. 2016
2. Peyron P, Vaubourgeix J, Poquet Y, Levillain F, Botanch C, Bardou F, Daffe M, Emile JF, Marchou B, Cardona PJ, de Chastellier C, Altare F. Foamy macrophages from tuberculous patients' granulomas constitute a nutrient-rich reservoir for *M. tuberculosis* persistence. PLoS Pathog. 2008; 4:e1000204. [PubMed: 19002241]
3. Lovewell RR, Sassetti CM, VanderVen BC. Chewing the fat: lipid metabolism and homeostasis during M. tuberculosis infection. Current opinion in microbiology. 2016; 29:30–36. [PubMed: 26544033]
4. Deb C, Daniel J, Sirakova TD, Abomoelak B, Dubey VS, Kolattukudy PE. A novel lipase belonging to the hormone-sensitive lipase family induced under starvation to utilize stored triacylglycerol in *Mycobacterium tuberculosis*. J Biol Chem. 2006; 281:3866–3875. [PubMed: 16354661]
5. Singh KH, Jha B, Dwivedy A, Choudhary E, Arpitha G, Ashraf A, Agarwal N, Biswal BK. Characterization of a secretory hydrolase from Mycobacterium tuberculosis sheds critical insight into host lipid utilization by M. tuberculosis. Journal of Biological Chemistry. 2017 jbc. M117. 794297.
6. West NP, Cergol KM, Xue M, Randall EJ, Britton WJ, Payne RJ. Inhibitors of an essential mycobacterial cell wall lipase (Rv3802c) as tuberculosis drug leads. Chem Commun (Camb). 2011; 47:5166–5168. [PubMed: 21384024]
7. Delorme V, Diomande SV, Dedieu L, Cavalier JF, Carriere F, Kremer L, Leclaire J, Fotiadu F, Canaan S. MmPPOX inhibits *Mycobacterium tuberculosis* lipolytic enzymes belonging to the hormone-sensitive lipase family and alters mycobacterial growth. PLoS One. 2012; 7:e46493. [PubMed: 23029536]
8. Ortega C, Anderson LN, Frando A, Sadler NC, Brown RW, Smith RD, Wright AT, Grundner C. Systematic Survey of Serine Hydrolase Activity in Mycobacterium tuberculosis Defines Changes Associated with Persistence. Cell Chem Biol. 2016; 23:290–298. [PubMed: 26853625]
9. Tallman KR, Levine SR, Beatty KE. Small-Molecule Probes Reveal Esterases with Persistent Activity in Dormant and Reactivating Mycobacterium tuberculosis. ACS Infect Dis. 2016; 2:936–944. [PubMed: 27690385]
10. Ravindran MS, Rao SP, Cheng X, Shukla A, Cazenave-Gassiot A, Yao SQ, Wenk MR. Targeting lipid esterases in mycobacteria grown under different physiological conditions using activity-based profiling with tetrahydrolipstatin (THL). Molecular & cellular proteomics: MCP. 2014; 13:435–448. [PubMed: 24345785]
11. Tallman KR, Levine SR, Beatty KE. Profiling Esterases in Mycobacterium tuberculosis Using Far-Red Fluorogenic Substrates. ACS Chem Biol. 2016; 11:1810–1815. [PubMed: 27177211]
12. Levine SR, Beatty KE. Synthesis of a far-red fluorophore and its use as an esterase probe in living cells. Chem Commun (Camb). 2016; 52:1835–1838. [PubMed: 26669746]
13. McKary MG, Abendroth J, Edwards TE, Johnson RJ. Structural basis for the strict substrate selectivity of the mycobacterial hydrolase LipW. Biochemistry. 2016; 55:7099–7111. [PubMed: 27936614]

14. Layre E, Sweet L, Hong S, Madigan CA, Desjardins D, Young DC, Cheng TY, Annand JW, Kim K, Shamputa IC, McConnell MJ, Debono CA, Behar SM, Minnaard AJ, Murray M, Barry CE 3rd, Matsunaga I, Moody DB. A comparative lipidomics platform for chemotaxonomic analysis of Mycobacterium tuberculosis. Chem Biol. 2011; 18:1537–1549. [PubMed: 22195556]
15. Layre E, Moody DB. Lipidomic profiling of model organisms and the world's major pathogens. Biochimie. 2013; 95:109–115. [PubMed: 22971440]
16. Kind T, Liu KH, doLee Y, DeFelice B, Meissen JK, Fiehn O. LipidBlast in silico tandem mass spectrometry database for lipid identification. Nat Methods. 2013; 10:755–758. [PubMed: 23817071]
17. Sartain MJ, Dick DL, Rithner CD, Crick DC, Belisle JT. Lipidomic analyses of Mycobacterium tuberculosis based on accurate mass measurements and the novel "Mtb LipidDB". J Lipid Res. 2011; 52:861–872. [PubMed: 21285232]
18. Stehr, M., Elamin, AA., Singh, M. Lipid inclusions in mycobacterial infections. INTECH Open Access Publisher; 2013.
19. Meniche X, Labarre C, de Sousa-d'Auria C, Huc E, Laval F, Tropis M, Bayan N, Portevin D, Guilhot C, Daffe M, Houssin C. Identification of a stress-induced factor of Corynebacterineae that is involved in the regulation of the outer membrane lipid composition. J Bacteriol. 2009; 191:7323–7332. [PubMed: 19801408]
20. Lavis LD, Chao TY, Raines RT. Synthesis and utility of fluorogenic acetoxymethyl ethers. Chem Sci. 2011; 2:521–530. [PubMed: 21394227]
21. Tian L, Yang Y, Wysocki LM, Arnold AC, Hu A, Ravichandran B, Sternson SM, Looger LL, Lavis LD. Selective esterase-ester pair for targeting small molecules with cellular specificity. Proc Natl Acad Sci USA. 2012; 109:4756–4761. [PubMed: 22411832]
22. Hedge MK, Gehring AM, Adkins CT, Weston LA, Lavis LD, Johnson RJ. The structural basis for the narrow substrate specificity of an acetyl esterase from *Thermotoga maritima*. Biochim Biophys Acta. 2012; 1824:1024–1030. [PubMed: 22659119]
23. Ellis EE, Adkins CT, Galovska NM, Lavis LD, Johnson RJ. Decoupled roles for the atypical, bifurcated binding pocket of the ybfF hydrolase. ChemBioChem. 2013; 14:1134–1144. [PubMed: 23670977]
24. Lukowski JK, Savas CP, Gehring AM, McKary MG, Adkins CT, Lavis LD, Hoops GC, Johnson RJ. Distinct substrate selectivity of a metabolic hydrolase from *Mycobacterium tuberculosis*. Biochemistry. 2014; 53:7386–7395. [PubMed: 25354081]
25. Johnson RJ, Hoops GC, Savas CJ, Kartje Z, Lavis LD. A sensitive and robust enzyme kinetic experiment using microplates and fluorogenic ester substrates. J Chem Educ. 2014; 92:385–388.
26. Prasanna AN, Mehra S. Comparative phylogenomics of pathogenic and non-pathogenic mycobacterium. PLoS One. 2013; 8:e71248. [PubMed: 24015186]
27. Dhouib R, Laval F, Carriere F, Daffe M, Canaan S. A monoacylglycerol lipase from Mycobacterium smegmatis Involved in bacterial cell interaction. J Bacteriol. 2010; 192:4776–4785. [PubMed: 20601476]
28. Singh G, Jadeja D, Kaur J. Lipid hydrolizing enzymes in virulence: *Mycobacterium tuberculosis* as a model system. Crit Rev Microbiol. 2010; 36:259–269. [PubMed: 20500016]
29. Farberg AM, Hart WK, Johnson RJ. The unusual substrate specificity of a virulence associated serine hydrolase from the highly toxic bacterium, *Francisella tularensis*. Biochem Biophys Rep. 2016; 7:415–422. [PubMed: 28955933]
30. Montoro-Garcia S, Gil-Ortiz F, Garcia-Carmona F, Polo LM, Rubio V, Sanchez-Ferrer A. The crystal structure of the cephalosporin deacetylating enzyme acetyl xylan esterase bound to paraoxon explains the low sensitivity of this serine hydrolase to organophosphate inactivation. Biochem J. 2011; 436:321–330. [PubMed: 21382014]
31. Målen H, Berven FS, Fladmark KE, Wiker HG. Comprehensive analysis of exported proteins from Mycobacterium tuberculosis H37Rv. Proteomics. 2007; 7:1702–1718. [PubMed: 17443846]
32. Lun S, Bishai WR. Characterization of a Novel Cell Wall-anchored Protein with Carboxylesterase Activity Required for Virulence in Mycobacterium tuberculosis. Journal of Biological Chemistry. 2007; 282:18348–18356. [PubMed: 17428787]

33. Zhao Q, Li W, Chen T, He Y, Deng W, Luo H, Xie J. Mycobacterium tuberculosis serine protease Rv3668c can manipulate the host–pathogen interaction via Erk-NF-κB axis-mediated cytokine differential expression. Journal of Interferon & Cytokine Research. 2014; 34:686–698. [PubMed: 24684623]
34. Dhouib R, Ducret A, Hubert P, Carriere F, Dukan S, Canaan S. Watching intracellular lipolysis in mycobacteria using time lapse fluorescence microscopy. Biochim Biophys Acta. 2011; 1811:234–241. [PubMed: 21238605]
35. Wu ML, Gengenbacher M, Dick T. Mild nutrient starvation triggers the development of a small-cell survival morphotype in mycobacteria. Frontiers in microbiology. 2016; 7
36. Garton NJ, Christensen H, Minnikin DE, Adegbola RA, Barer MR. Intracellular lipophilic inclusions of mycobacteria in vitro and in sputum. Microbiology. 2002; 148:2951–2958. [PubMed: 12368428]
37. Wittig I, Schagger H. Features and applications of blue-native and clear-native electrophoresis. Proteomics. 2008; 8:3974–3990. [PubMed: 18763698]
38. Saminathan M, Muthukumaresan KT, Rengarajan S, Muthukrishnan N, Gautam P. Blue native electrophoresis study on lipases. Anal Biochem. 2008; 377:270–271. [PubMed: 18381198]
39. Komatsu T, Hanaoka K, Adibekian A, Yoshioka K, Terai T, Ueno T, Kawaguchi M, Cravatt BF, Nagano T. Diced electrophoresis gel assay for screening enzymes with specified activities. J Am Chem Soc. 2013; 135:6002–6005. [PubMed: 23581642]
40. Rawat M, Heys J, Av-Gay Y. Identification and characterization of a diamide sensitive mutant of Mycobacterium smegmatis. FEMS microbiology letters. 2003; 220:161–169. [PubMed: 12670676]
41. Ortega C, Anderson LN, Frando A, Sadler NC, Brown RW, Smith RD, Wright AT, Grundner C. Systematic Survey of Serine Hydrolase Activity in Mycobacterium tuberculosis Defines Changes Associated with Persistence. Cell chemical biology. 2016; 23:290–298. [PubMed: 26853625]
42. Choudhary E, Thakur P, Pareek M, Agarwal N. Gene silencing by CRISPR interference in mycobacteria. Nat Commun. 2015; 6:6267. [PubMed: 25711368]
43. Rock JM, Hopkins FF, Chavez A, Diallo M, Chase MR, Gerrick ER, Pritchard JR, Church GM, Rubin EJ, Sassetti CM, Schnappinger D, Fortune SM. Programmable transcriptional repression in mycobacteria using an orthogonal CRISPR interference platform. Nat Microbiol. 2017; 2:16274. [PubMed: 28165460]
44. Larsen EM, Stephens DC, Clarke NH, Johnson RJ. Ester-prodrugs of ethambutol control its antibacterial activity and provide rapid screening for mycobacterial hydrolase activity. Bioorg Med Chem Lett. 2017; 27:4544–4547. [PubMed: 28882482]
45. Babicki S, Arndt D, Marcu A, Liang Y, Grant JR, Maciejewski A, Wishart DS. Heatmapper: web-enabled heat mapping for all. Nucleic Acids Res. 2016; 44:W147–153. [PubMed: 27190236]

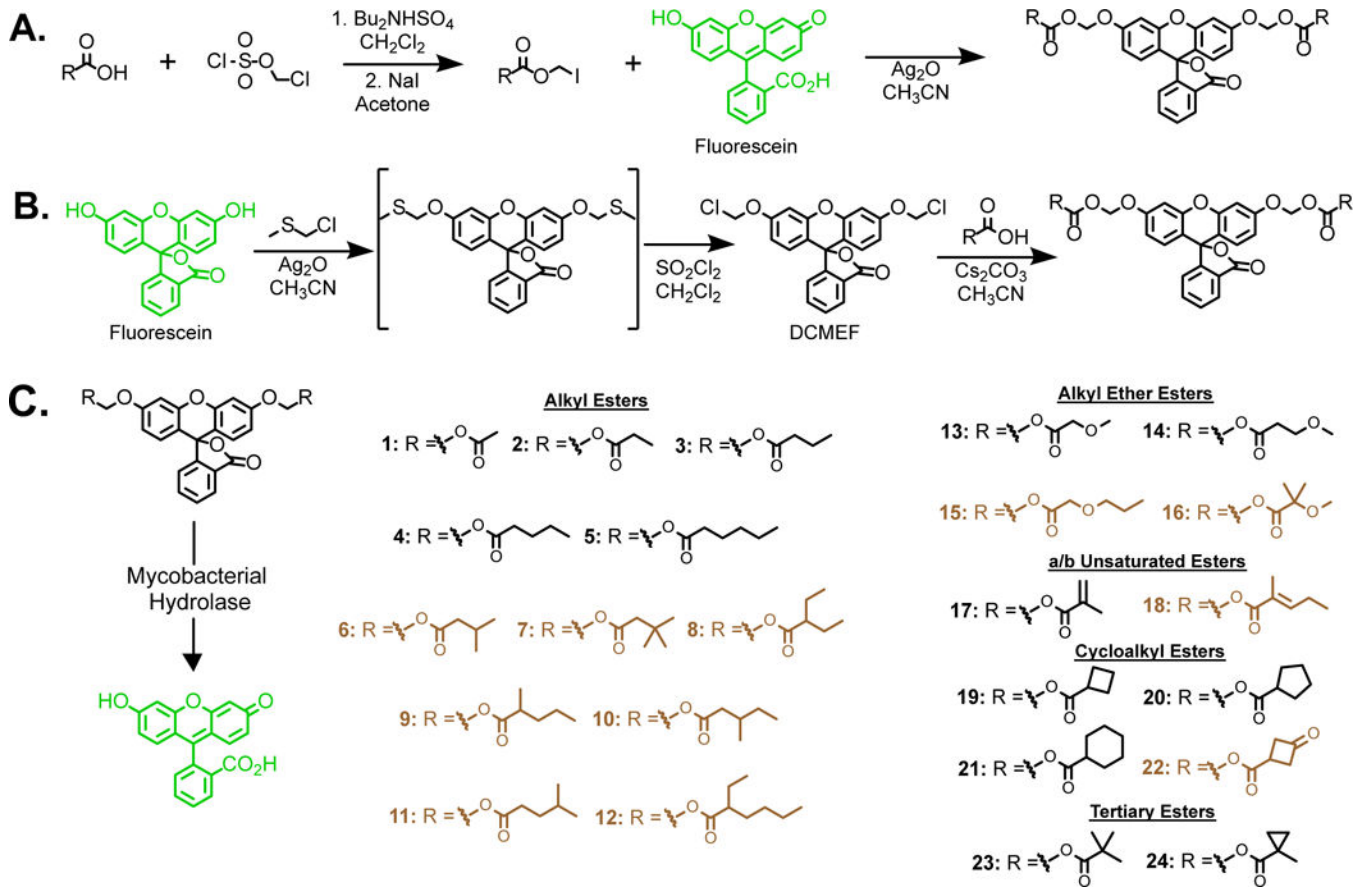

Figure 1. Fluorogenic substrate library

(A) Previous published synthesis of acyloxymethyl ether fluorescein derivatives.[20, 23] Due to the complexity of separating the various ether-ester byproducts, yields from this synthetic reaction are fairly low. (B) Revamped synthesis. The intermediate dichloromethyl ether fluorescein (DCMEF) can be produced in high yields, is stable long-term, and can be derivatized in one step. (C) Expanded substrate library. Substrates are grouped based on structure activity relationships. Novel substrates synthesized for this work are shown in brown. Substrates added to mimic the natural diversity of mycobacterial lipids and esters, include branched (**6** – **12**; **18**) and polar (**13** – **16**; **22**) esters.[14–17]

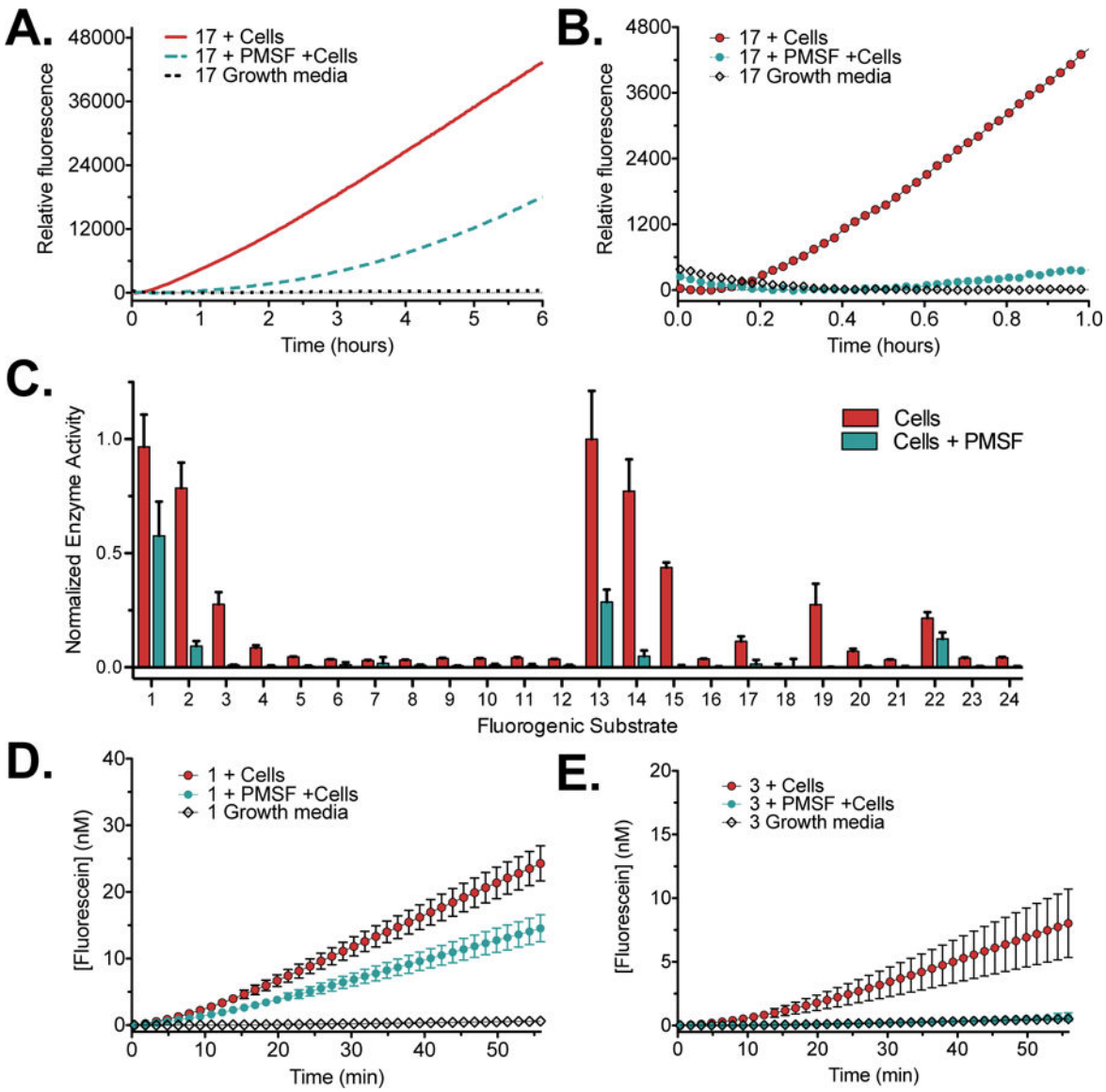

Figure 2. Global substrate specificity of mycobacterial serine hydrolases

(A) Incubation of substrate **17** with actively growing *M. smegmatis* for 6 hours with fluorescent detection of substrate activation (Ex 480 nm; Em 510 nm). Control reactions were completed with *M. smegmatis* in the presence of 1 mM PMSF and in growth media alone. (B) Substrate **17** activation was quantified for 1 h. Additional fluorogenic substrate activations were completed for 1 h. Only a single fluorogenic reaction is shown in A and B to illustrate the raw activation profile in actively growing *M. smegmatis*. For each substrate, this reaction was then completed in triplicate with two biological replicates and averaged for Figure 2C. (C) Global SAR of mycobacterial hydrolases in the presence of actively growing *M. smegmatis*. Hydrolysis rates were measured for 1 h at 37 °C in solutions containing substrate and *M. smegmatis* cultures at OD_{600} = 0.045. PMSF (1 mM) was added at a sub-inhibitory concentration. Normalized enzyme activity (± SE) is shown where the highest activity substrate was given a value of 1.0 and other enzyme activities were normalized in

relation to this highest activity substrate based on steady state rate (nM/min). Results are the average of at least triplicate fluorescent measurements for two separate biological replicates. (D and E) Differential inhibition of mycobacterial hydrolases by PMSF. Fluorogenic activation measured over 1 hour identically to 2C. A fluorescein standard curve completed in triplicate on the same plate was used to convert relative fluorescence into [fluorescein]. Relative activity of substrates **1** (D) and **3** (E) in the absence and presence of PMSF. Additional substrate data are shown in Figure S1.

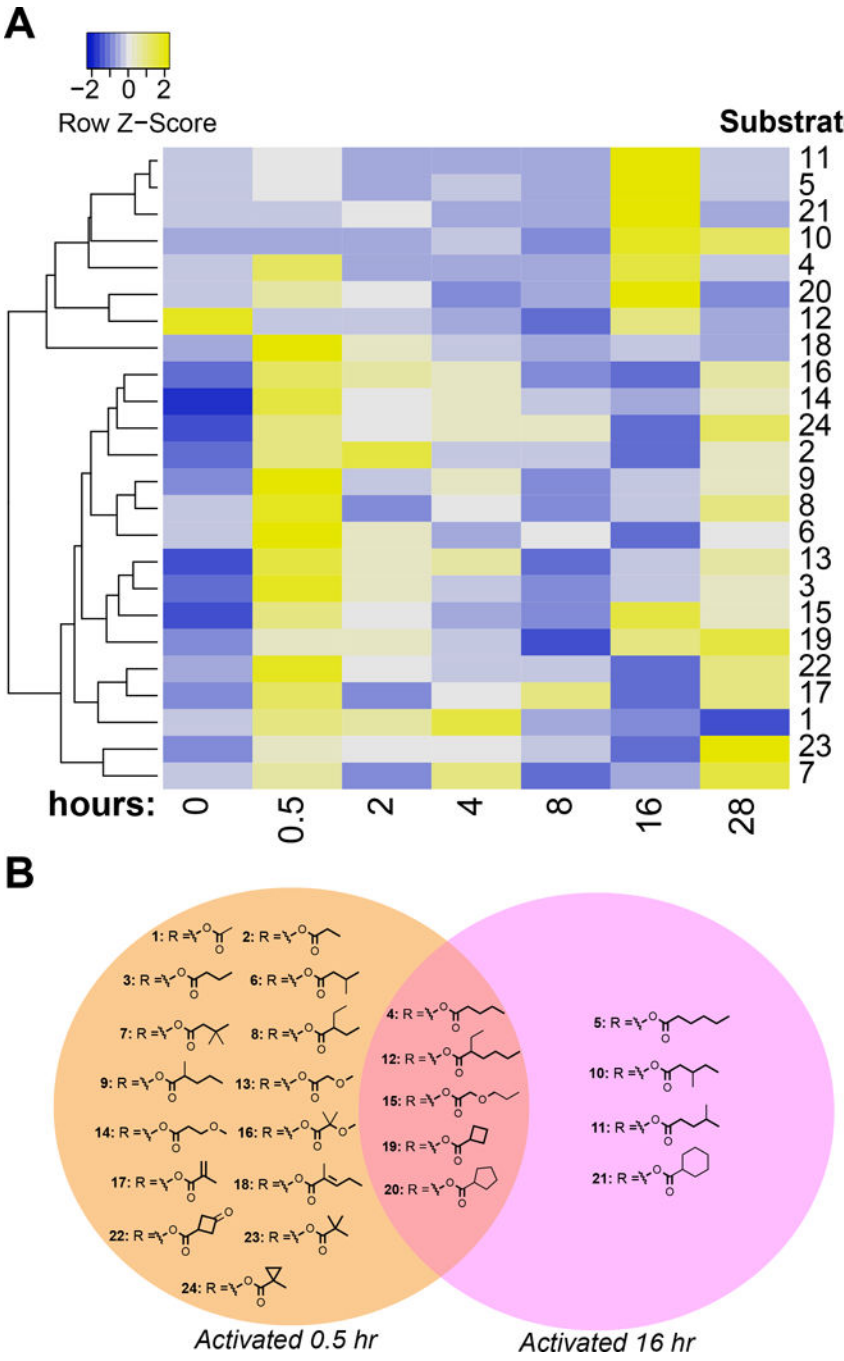

Figure 3. Shifts in hydrolase activity under nutrient starvation conditions

(A) Activation normalized to the timepoint at which the highest activity was observed for each substrate. Heat map constructed using Heatmapper with clustering based on complete linkage and distance based on Euclidean distance measurements.[45] Actively growing *M. smegmatis* cultures were pelleted, resuspended in PBS, incubated at 37 °C with rapid shaking (225 RPM) for the nutrient depravation time (30 min – 28 h), and lysate was prepared (Figure S3). Results are the average of at least triplicate fluorescent measurements for two separate biological replicates. (B) SAR based on shifts in hydrolase activity under

various time points post nutrient starvation. Substrate activation grouped based on highest activation at 0.5 hr, 16 hr, or overlapping activation at these two time points.

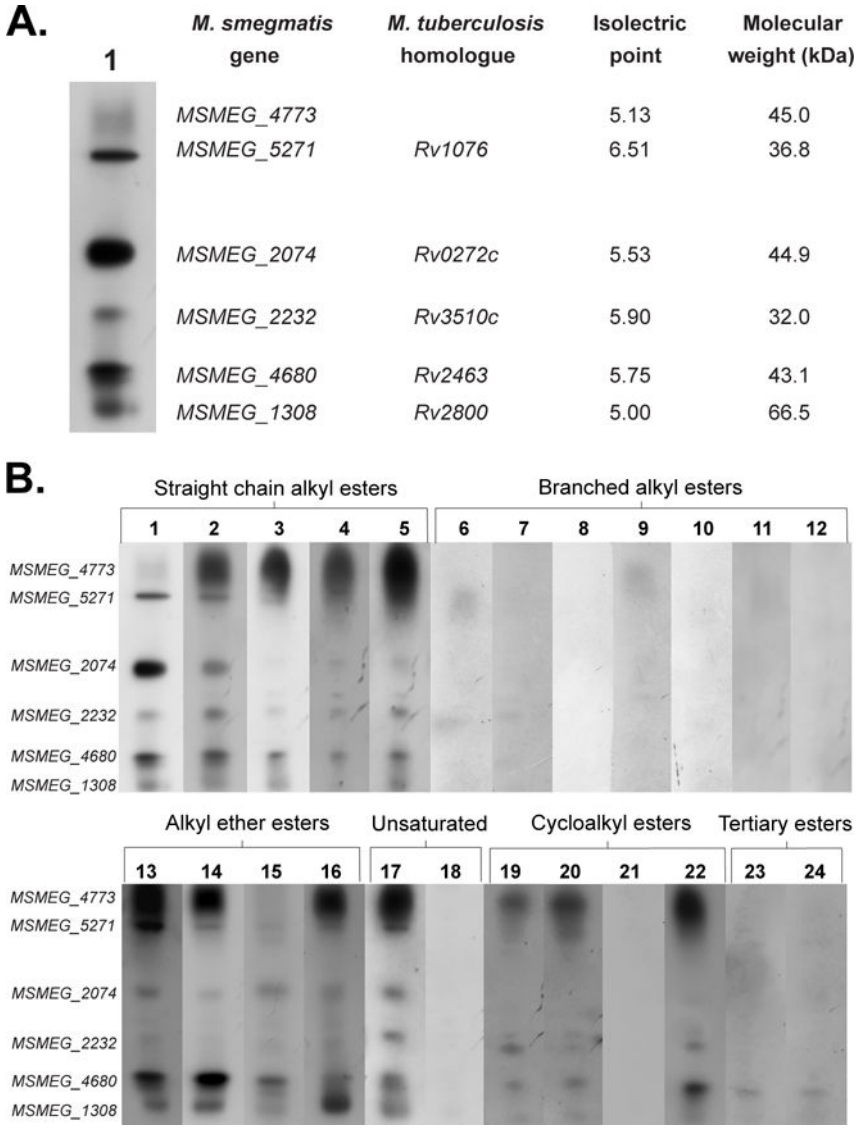

Figure 4. Identification of *M. smegmatis* enzymes under standard growth conditions

M. smegmatis lysate (12 μg) was loaded into a native-PAGE gel (4-20%) and separated at 200 V for 90 min. (A) The native-PAGE gel was exposed to substrate **1** for 45 min and images were obtained using a fluorescent imager.[3,6] The resulting bands were excised and LC-MS/MS performed.[3] (B) Global in-gel hydrolase activity. Gels were exposed to the fluorophores for varying amounts of time (20 min for substrates **13**-**15**; 45 min for substrates **1**-**2**, **22**; and 60 min for all remaining substrates) and relative activation measured using a fluorescent imager. Results are representative of the two biological replicates. Protein bands identified in Figure 4A are labelled along with the subclassifications of fluorogenic substrates (Figure 1C).